Phase Holdups in Three-Phase Fluidized Beds

The local bubble frequency, the local phase holdups and the local bed porosity in three-phase fluidized beds were measured. Air, water, and 250 μm glass beads were used as the gas, liquid, and solid phases. The effects of gas and liquid velocities on phase holdups were studied. Time-averaged local gas holdup and bubble frequency were measured by an optical fiber probe. Mass balances were performed at various axial positions along the fluidized beds to check the accuracy of the measurements.

S. L. P. Lee, H. I. de Lasa
Faculty of Engineering Science
University of Western Ontario
London, Ontario, Canada N6A 5B9

Introduction

Three-phase fluidization is an operation used to bring into contact gas, liquid, and solid particles. The solid particles are fluidized by upflow liquid, which is the continuous phase, and cocurrent dispersed gas bubbles. Three-phase fluidization has received great attention in the past few decades because it has been applied in many chemical processes (Bickel and Thomas, 1982; Blum and Toman, 1977; Deckwer, 1980; Hellwig et al., 1966; Mounce and Rubin, 1971; Rapp and van Drisen, 1965; Smith et al., 1978).

The characteristics of three-phase fluidized bed (TPFB) reactors have been reviewed by Baker (1981), de Lasa and Lee (1986), Epstein (1981), Muroyama and Fan (1986), Ostergaard (1971), and Wild (1983).

An interesting phenomenon is the bed expansion or contraction upon injecting gas into a liquid fluidized bed while the liquid flow rate is kept constant. With large particles, the bed height increases monotonically as gas velocity increases. However, an initial decrease of bed height exists if small particles are used. This phenomenon is believed to be caused by the wake trailing behind the bubble.

The phenomenon of bubble wake was also studied by various investigators. Due to the lack of experimental data, certain key parameters, such as the solid concentration in the wake and the wake size, were not available. Iterative methods were proposed to assess the parameters of the models. In order to carry out the computation, an assumption has to be made to estimate the solid concentration in the wake. Efremov and Vakhrushev (1970), Darton and Harrison (1976), and Baker et al. (1977) assumed that the wake was free of solid. Ostergaard (1965) assumed that the solid concentration in the wake was the same as that in the particulate phase. A generalized assumption of wake solid concentration varing within these two extremes was used by Bhatia and Epstein (1974), and El-Temtamy and Epstein (1978).

The bed porosity and the individual phase holdups in TPFB have been investigated by Armstrong et al. (1976), Bhatia et al. (1972), Dakshinamurty et al. (1971, 1972), Kim et al. (1972, 1975), Razumov et al. (1973, 1977), Soung (1978), and Vail et al. (1970). In the conventional study of phase holdups and bed porosity, overall values are obtained through the pressure profile along the fluidized bed, the total amount of solid particles, and the continuity of the three phases. In addition, the phase holdups are assumed to be uniform in the bed.

In order to obtain information on local phase holdups, *in situ* measuring probes have been used in various studies (Begovich and Watson, 1978a, b; Dhanuka and Stepanek, 1978; Lee et al., 1984; Linnewber and Blass, 1983; Morooka et al., 1982; Rigby et al., 1970). It is inevitable that the hydrodynamics of the fluidized bed is somewhat disrupted by an *in situ* measuring device. Therefore, one has to be cautious in the design of *in situ* probes so that the disturbance to the hydrodynamics can be minimized. In any case, the results obtained from *in situ* probe measurements indicate that there are variations of phase holdups in both the axial and the radial directions in a TPFB, particularly in the top section of the bed. For example, the solid holdup in that region decreased gradually until the gas-liquid freeboard region was reached (solid free).

The performance of a TPFB reactor is highly influenced by the hydrodynamic properties such as the phase holdups. For example, the design of a TPFB reactor depends on the expansion/contraction of the fluidized bed, which is in turn affected by the bed porosity. The bubble size, gas residence time, and consequently the gas-liquid mass transfer are influenced by the phase holdups. Therefore the bed porosity and the phase holdups are among the important information needed for the design of a TPFB reactor.

Most of the research on TPFB's has been carried out in beds of large solid particles even though TPFB's with small particles

are also of interest in chemical industry. Therefore, narrow cut glass beads of 250 μm dia. were chosen in this study. The objectives of the present work were to measure the local phase holdups and to study the effect of operating conditions on phase holdups in three-phase fluidized beds. In order to have an adequate assessment of phase holdups and their variations with position, local gas holdup was measured throughout the fluidized bed both in axial and in radial directions.

The global and the local phase holdups in three-phase fluidized beds were studied experimentally. The liquid and the gas holdups were influenced by both the gas and the liquid velocities, while the bed porosity was mainly affected by the liquid velocity. A response surface method was applied successfully in correlating the bed porosity data of two-phase (liquid-solid) and three-phase (gas-liquid-solid) fluidized beds.

The local gas holdup was measured by an optical fiber probe. The jet effect was quite noticeable near the inlet grid; however, the gas bubbles dispersed and redistributed rapidly. Once above the grid region, parabolic radial profiles of gas holdups were observed in most of the experiments performed. In the axial direction, the gas holdup increased slightly with height. The solid and the liquid holdups were fairly constant in the lower two-thirds of the fluidized bed. In the top region of the bed, the solid holdup decreased rapidly and the liquid holdup increased correspondingly. Concerning the freeboard region, a new approach was demonstrated for the study of particle entrainment.

Experimental Apparatus

The experiments were carried out in a cylindrical column of 0.2 m ID and 3.35 m height. Glass beads of 250 μm dia. were used as solid particles. Tap water was used as the major fluidizing medium, which was the continuous phase, and air was dispersed in the liquid fluidized bed. A flow diagram of the system is shown in Figure 1. Water was withdrawn from the storage tank to a centrifugal pump. The outlet stream from the pump was split into two; one stream was recycled back to the tank, while the other was measured by a flowmeter and fed to the fluidized bed. Air was measured by flowmeters before it was injected into the bed. Water and air bubbles rose through the fluidized bed and the freeboard region and were separated in the disengaging section.

The fluidized bed apparatus consisted of three sections. The first was the liquid distributing section, which insured an even distribution of liquid. A manifold with three injectors was mounted at the bottom of the distribution box. In order to have even distribution of liquid flow, a perforated plate was placed on top of the distribution box. On the plate, there were 54 holes 1.6 mm dia. arranged evenly in triangular pitches of 25.4 mm.

The second section was the fluidized bed testing section, where the bubble measuring probes could be positioned at various radial and axial positions in the fluidized bed. The third section of the system was the gas-liquid disengaging section, where the liquid was collected and recycled to the storage tank. Air bubbles were injected into the column through four 0.94 cm gas nozzles. These injectors were mounted on the bottom of the plate and were distributed as follows: one at the center, and the other three 6.78 cm from the center with 120° circumferential separation. A stainless steel screen was attached to the perforated plate distributor to prevent solid from leaking through the grid into the liquid distribution box. From the inlet grid and up, there were 36 pressure taps mounted on the column walls with equal spacing of 50.8 mm. At the very top of the column, there were another six pressure taps that were separated evenly with spacing of 102 mm. In order to prevent solid particles from entering the pressure measurement lines, a stainless steel screen was soldered at the tip of each pressure tap. Static pressures were mea-

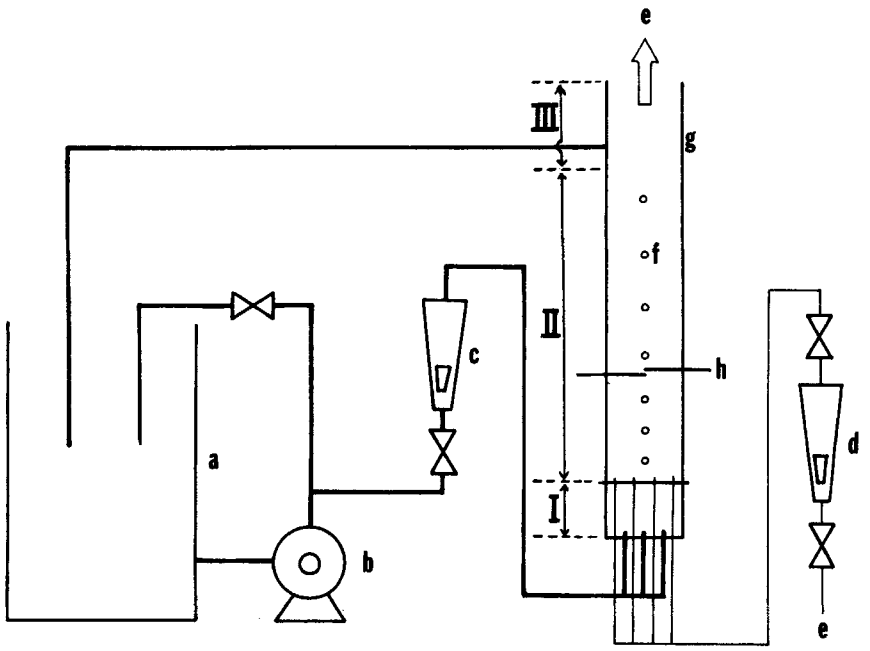

Figure 1. Experimental set-up.

a. Liquid storage tank
b. Centrifugal pump
c,d. Flowmeters
e. Air
f. Pressure taps
g. Column
h. Optical fiber probes

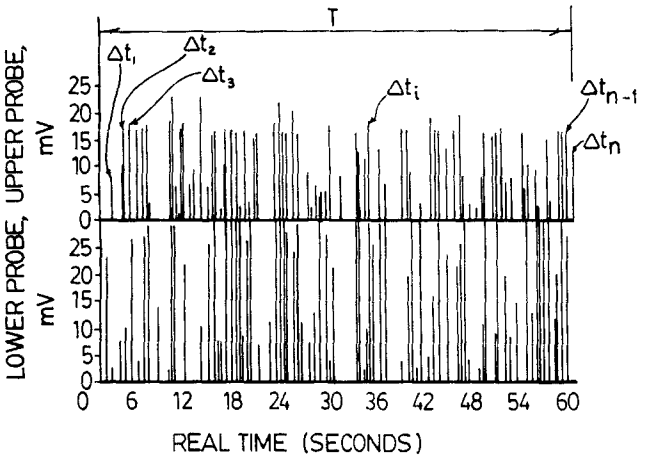

Figure 2. Typical signals of bubble measurements.

sured by a pressure transducer with a mechanical switch wafer device (Scanivalve). These static pressure profiles were used as described in the following sections for assessing the holdups of the different phases in the bed. For the various experiments conducted, the settled bed height was kept constant at about 43 cm.

Bubble Measuring System

In order to obtain the local phase holdups, an *in situ* optical fiber probe was used to measure the gas holdup directly. A single-core silica optical fiber of 400 μm was bent to a U shape. The detection of gas bubbles took place at the turning point. The radius of the U at the tip of the probe was approximately 0.5 mm. The optical fiber was sealed inside a stainless steel tube and only the top of the U bend was exposed. The detailed design of the probe and the measuring system were described in previous publications (de Lasa et al., 1984; Lee et al., 1986; Lee, 1986).

The time-averaged local gas holdup can be obtained through analysis of the signal from the optical probe. Figure 2 is an example historical diagram of the probe response during measurement. In the case shown here, two optical probes were used, separated vertically with a distance of 0.94 cm between. The gas holdup can be assessed by counting the fraction of time occupied by the gas bubbles.

$$\epsilon_g = \frac{\sum_{i=1}^{n} \Delta t_i}{T} \tag{1}$$

In order to get representative results, stationary tests were performed to determine the minimum time required to ensure that the data taken were obtained under stationary conditions in terms of statistical analysis (Bendat and Piersol, 1966, 1980). The stationary test was performed by comparing two sets of data of the same sampling time under the same operating condition. The mean value, the root mean square, and the standard deviation of each data set were calculated for comparison. A sampling time of 90 s was found to be acceptable. Some results of the stationary tests are listed in Table 1, where the deviations of mean value, RMS, and standard deviation between the two sets of data are shown. In the systematic experiments for gas holdup, a sampling time of 110 s was used so as to have even better stationary properties of the data.

Analysis of Phase Holdups

The overall phase holdups in a three-phase fluidized bed can be obtained through the following equations.

$$-\Delta P = g(\epsilon_L \rho_L + \epsilon_G \rho_G + \epsilon_S \rho_S) H_b \tag{2}$$

$$\epsilon_L + \epsilon_G + \epsilon_S = 1 \tag{3}$$

$$\epsilon_S = M_S/(H_b A \rho_S) \tag{4}$$

The fluidized bed height can be obtained either by visual observation or by the pressure gradient method. This method of

Table 1. Stationary Test

V_G mm/s	V_L mm/s	Z m	r/R	Data Set*	Mean Value mV	Dev. of Mean Value %	RMS mV	Dev. of RMS %	Std. Dev. mV	Dev. of Std. Dev. %
12.8	3.9	0.525	0	a	231.3	+0.087	232.1	+0.086	18.66	+0.11
12.8	3.9	0.525	0	b	230.9	−0.087	231.7	−0.086	18.70	−0.11
12.8	3.9	0.525	0.75	a	224.3	−0.16	224.6	−0.20	14.34	−6.03
12.8	3.9	0.525	0.75	b	225.0	+0.16	225.5	+0.20	16.18	+6.03
12.8	15.6	0.525	0	a	224.5	−0.22	225.9	−0.26	26.19	−3.22
12.8	15.6	0.525	0	b	225.5	+0.22	227.1	+0.26	27.93	+3.22
12.8	15.6	0.525	0.75	a	222.3	−0.18	222.7	−0.067	14.63	+2.05
12.8	15.6	0.525	0.75	b	222.7	+0.18	223.0	+0.067	14.04	−2.05
20.0	3.9	0.525	0	a	231.0	+0.087	232.3	+0.13	25.11	+3.64
20.0	3.9	0.525	0	b	230.6	−0.087	231.7	−0.13	23.35	−3.64
20.0	3.9	0.525	0.75	a	232.6	+0.30	233.5	+0.32	20.69	+1.49
20.0	3.9	0.525	0.75	b	231.2	−0.30	232.0	−0.32	20.08	−1.49
20.0	15.6	0.525	0	a	240.4	−0.35	241.9	−0.47	27.23	−8.64
20.0	15.6	0.525	0	b	242.1	+0.35	244.2	+0.47	32.38	+8.64
20.0	15.6	0.525	0.75	a	235.2	−0.021	235.9	0.00	19.59	+4.95
20.0	15.6	0.525	0.75	b	235.3	+0.021	235.9	0.00	17.74	−4.95

*Sampling time of each data = 90 s.

phase holdup measurement is based on the assumption of a homogeneous fluidized bed. In other words, it is assumed that there is no axial or radial variation of phase holdup. In reality, there are significant variations of phase holdups in a TPFB, particularly at high fluidizing velocities. In addition, when high fluidizing velocities are used the surface of the fluidized bed becomes ambiguous and fluctuant. In this case a higher level of error is involved in the use of Eq. 4.

Local phase holdups have to be measured in order to have more realistic phase holdup information. In the present work the local gas holdup was measured directly by the optical probe at various axial and radial positions. The cross-sectional average gas holdup at a fixed axial height was calculated by the following equation:

$$\epsilon_g = \frac{1}{\pi R^2}\int_0^R \epsilon_{gr} 2\pi r \, dr \tag{5}$$

Once the cross-sectional average gas holdup is available, the local liquid and solid holdups at a fixed axial position can be obtained by using Eq. 3 and the local pressure at that particular axial height in the fluidized bed.

$$-\frac{dP}{dZ} = g(\epsilon_l \rho_l + \epsilon_g \rho_g + \epsilon_s \rho_s) \tag{6}$$

Results and Discussion

The average liquid holdups in three-phase fluidized beds are shown in Figure 3. The liquid holdup was affected by both the liquid and the gas velocities, but the latter had less influence. A higher liquid velocity resulted in a higher liquid holdup, while the gas velocity had the reverse effect. Two different models were used in the regression analysis to correlate the data of liquid holdup. The first model, Eq. 7, was the commonly used power law model, the second, Eq. 8, was the exponential model:

$$\epsilon_L = 0.006\, V_L^{0.246} V_G^{-0.059} \tag{7}$$

with standard deviation of 0.009, and

$$\epsilon_L = 1 - 0.535 \exp(-0.378 V_L + 0.093 V_G) \tag{8}$$

with standard deviation of 0.014.

The predictions by Eqs. 7 and 8 are shown in Figure 3 as solid and dashed lines, respectively. Both Eq. 7 and Eq. 8 provided reasonable fitting of the data, while the former gave better predictions. However, the power law correlation is not suitable for extrapolation to low gas and/or liquid velocities. In any case, the predictions by either model are within ±5% error with respect to the experimental data.

The bed porosity is defined as the sum of gas and liquid holdups. The experimental data of bed porosity are shown in Figure 4. The bed porosity increased significantly with liquid velocity, while the gas velocity had very limited influence. Both the power law and the exponential models were attempted in the regression analysis.

$$\epsilon = 0.659\, V_L^{0.205} V_G^{0.006} \tag{9}$$

with standard deviation of 0.010, and

$$\epsilon = 1 - 0.531 \exp(-0.418 V_L - 0.004 V_G) \tag{10}$$

with standard deviation of 0.006.

The predictions by Eqs. 9 and 10 are shown in Figure 4 as dashed and solid lines, respectively. The predictions by either equation are well within ±4% error; Eq. 10 gives better fitting of the experimental data and also extrapolates better to low flow rates.

A unique phenomenon in three-phase fluidization is bed contraction/expansion when gas is introduced into a liquid-fluidized bed. Some experiments with a two-phase liquid-fluidized bed were also performed in this study. The fluidized bed heights were obtained from the analysis of pressure profiles along the bed and the bed porosities (liquid only) were calculated. The experimental data of bed porosity of both the liquid-solid and the three-phase fluidized beds are shown in Figure 5. Since small particles were used, initial bed contraction was observed in the range of low gas velocity and bed expansion took place when high gas velocity was used. The phenomenon of bed contraction

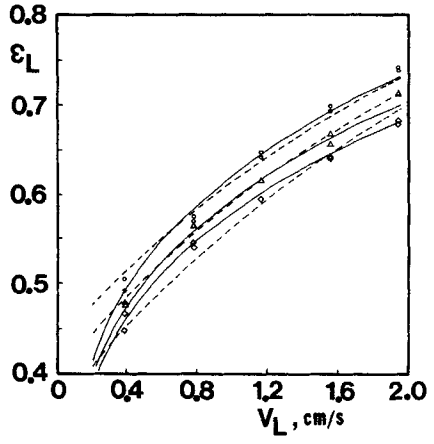

Figure 3. Effects of gas and liquid velocities on liquid holdup.

○ V_G = 5.7 mm/s — Eq. 7
△ V_G = 12.1 mm/s --- Eq. 8
◇ V_G = 19.0 mm/s

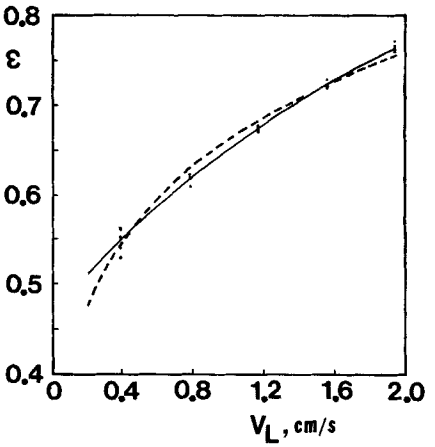

Figure 4. Effects of liquid and gas velocities on bed porosity.

---- Eq. 9; — Eq. 10
V_G between 5.7 and 19.0 mm/s

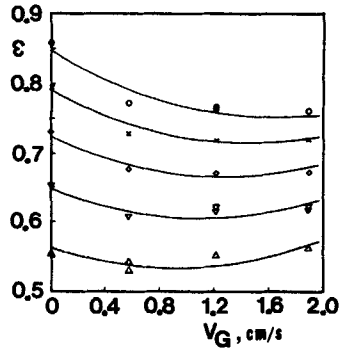

Figure 5. Effects of gas and liquid velocities on bed porosity.

△ V_L = 3.9 mm/s ▽ V_L = 7.9 mm/s
◇ V_L = 11.7 mm/s × V_L = 15.6 mm/s
○ V_L = 19.5 mm/s — Eq. 11

became more noticeable when higher liquid velocity was employed. This indicates that the bed contraction is affected by both the gas and the liquid velocities and there is a cross-linkage between these two factors. Therefore, a response surface methodology was applied in the data analysis and the following equation was obtained:

$$\epsilon = 0.470 + 0.253 V_L - 0.053 V_G - 0.030 V_L^2 + 0.036 V_G^2 - 0.033 V_L V_G \quad (11)$$

with standard deviation of 0.009.

The predictions by Eq. 11 are shown as solid lines in Figure 5. The accuracy of the predictions is within ±3% of the experimental data. Canonical analysis was used to reform Eq. 11 and the following equation was obtained:

$$\epsilon - 0.794 = 0.040 X_1^2 - 0.034 X_2^2 \quad (12)$$

where

$$X_1 = 0.409(V_L - 3.01) - 0.913(V_G - 2.12)$$

$$X_2 = 0.973(V_L - 3.01) - 0.229(V_G - 2.12)$$

A contour plot is shown in Figure 6 to illustrate the effects of gas and liquid velocities on bed porosity.

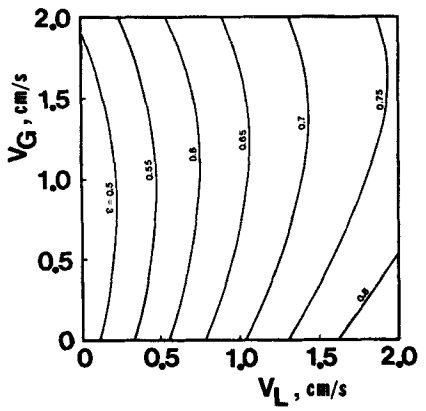

Figure 6. Contour map of bed porosity.

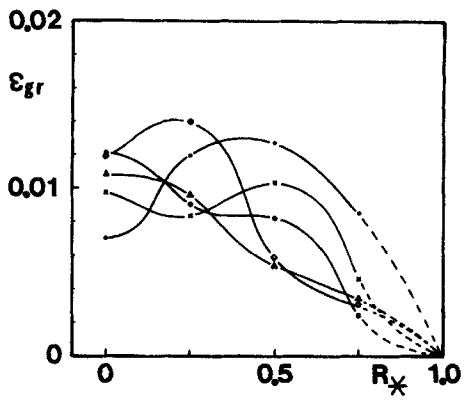

Figure 7. Effect of liquid velocity on radial gas hold-up profiles, Z = 0.525 m, V_G = 5.7 mm/s.

× V_L = 7.9 mm/s ○ V_L = 11.7 mm/s
△ V_L = 15.6 mm/s ◇ V_L = 19.5 mm/s
● V_L = 3.9 mm/s

An interesting fact can be observed when the extrapolations of Eqs. 8, 10, and 11 are taken to the limit of zero gas and liquid velocities. In these cases, the extrapolated values represent essentially the voidage of a packed bed of solid particles. The predictions by Eqs. 8, 10, 11 are respectively 0.465, 0.469, and 0.470. All these voidage estimations are very close to 0.4765, the maximum voidage of a packed bed of uniform spheres. These observations are quite logical because they are an extrapolation from fluidized beds. Since the solid particles used in this study were narrow-cut glass beads, the ideal assumption of uniform spheres should be adequate. Therefore, it is quite reasonable to observe that the extrapolated values are very close to 0.4765. Furthermore, these extrapolated values are a little smaller than the maximum bed voidage. This reveals the fact that there is some deviation from ideality for the particles used.

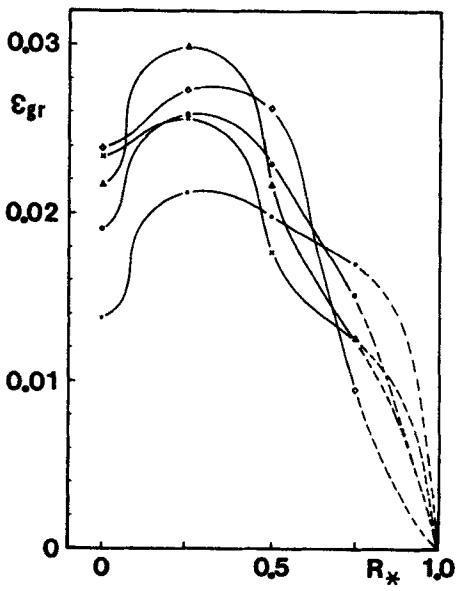

Figure 8. Effect of liquid velocity on radial gas holdup profiles, Z = 0.525 m, V_G = 12.1 mm/s.

● V_L = 3.9 mm/s × V_L = 7.9 mm/s
○ V_L = 11.7 mm/s △ V_L = 15.6 mm/s
◇ V_L = 19.5 mm/s

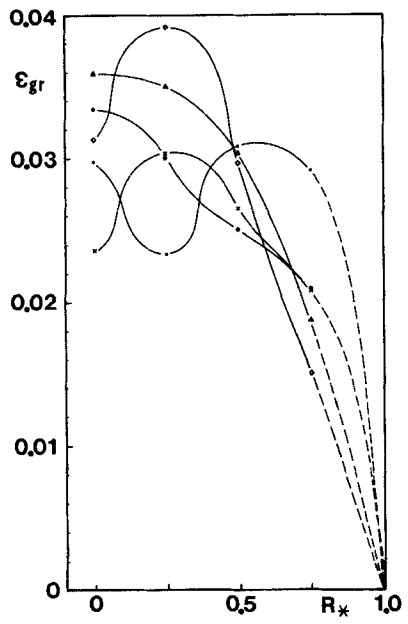

Figure 9. Effect of liquid velocity on radial gas holdup profiles, $Z = 0.525$ m, $V_G = 19.0$ mm/s.

● V_L = 3.9 mm/s × V_L = 7.9 mm/s
○ V_L = 11.7 mm/s △ V_L = 15.6 mm/s
◇ V_L = 19.5 mm/s

The effects of the gas and the liquid velocities on radial gas holdup profiles at a fixed axial position, $Z = 0.525$ m, are shown in Figures 7, 8, and 9. Measurements of gas holdups were performed at four different radial positions, $r/R = 0$, 0.25, 0.5, and 0.75. The gas holdup profiles were nearly flat across the bed for low liquid velocities. As the liquid velocity increased, higher gas holdups were observed around the center of the bed while lower gas holdups were found near the wall of the column. In other words, bell-shaped or double bell-shaped gas holdup profiles developed as the liquid velocity increased. The effect of liquid velocity on radial gas holdup profile was more pronounced when higher gas velocity was used. These observations indicate that gas bubbles tend to rise in the center at high liquid velocities. It was also found that the gas velocity had a profound influence on the gas holdup. For instance, at a constant liquid velocity the gas holdup increased considerably with gas velocity, as shown in Figures 7, 8, and 9.

The radial gas holdup and the bubble frequency profiles in three-phase fluidized beds were also studied thoroughly at various axial heights of the bed. The experiments were carried out at 0.075, 0.225, 0.375, 0.525, 0.675, and 0.825 m above the distributor. An example of the radial and the axial profiles of gas holdup in the fluidized bed is shown in Figure 10 for $V_G = 12.8$ mm/s and $V_L = 3.9$ to 15.6 mm/s. Similar results were also obtained for other operating conditions: $V_G = 20$ mm/s and $V_L = 3.9$ to 19.5 mm/s (Lee, 1986). It was observed that the jet effect was quite noticeable at the grid level, $Z = 0.075$ m. However, the gas bubbles dispersed and redistributed rapidly and the gas holdup profiles were found stabilized at higher axial positions. Once above the grid region, the radial gas holdup profiles at different axial levels were very similar and the gas holdups increased only slightly with height. This phenomenon became more noticeable as the liquid velocity increased, especially at very high fluidizing velocities.

In order to interpret the experimental data, the response surface method was applied to study the gas holdup profiles both axially and radially in the fluidized beds. The dimensionless axial and radial positions were considered to be the two independent variables in the model, and the experimental data obtained under different operating conditions were analyzed separately. The format of the model used is shown in the following equation:

$$\epsilon_{gr} = 10^{-2}(a_1 + a_2 Z_* + a_3 R_* + a_4 Z_*^2 + a_5 R_*^2 + a_6 Z_* R_*) \quad (13)$$

The results of the analyses are listed in Table 2, which includes the various coefficients and the standard deviations. In general, the radial profiles of gas holdup can be described by a parabolic type of function with the maximum at or near the center of the fluidized bed. Similar radial gas holdups in a TPFB with large particles were also observed by Linneweber and Blass (1983), Rigby et al. (1970), and Hu et al. (1986).

The prediction of gas holdups by Eq. 13 at various axial and radial positions is illustrated in Figure 10 by the solid lines. It was noticed that there was a sudden increase in gas holdup near the top of the fluidized bed. Such a phenomenon can be seen in the case shown in Figure 10a, where the highest axial position is only about 4 cm below the surface of the fluidized bed. This phenomenon can be explained by the fact that the solid holdup near the top of the bed is lower than the rest of the fluidized bed. A lower solid holdup gives a lower apparent bed viscosity, which

Table 2. Response Surface Analysis of Gas Holdup Profiles

$$\epsilon_{gr} = 10^{-2} \cdot (a_1 + a_2 Z_* + a_3 R_* + a_4 Z_*^2 + a_5 R_*^2 + a_6 Z_* R_*)$$

Gas Veloc. mm/s	Liquid Veloc. mm/s	a_1	a_2	a_3	a_4	a_5	a_6	Std. Dev. × 10^3
12.8	3.9	2.437	−3.559	1.766	3.608	−3.622	0.293	4.676
12.8	7.9	2.837	−2.617	−1.097	2.947	−1.464	0.405	2.569
12.8	11.7	3.188	−1.247	0.534	0.619	−4.136	1.562	2.742
12.8	15.6	2.383	1.209	0.875	−0.014	−3.645	0.580	2.898
20.0	3.9	4.722	−8.854	1.887	7.283	−4.548	0.065	6.253
20.0	7.9	1.148	6.700	0.786	−4.391	−3.296	−1.319	2.609
20.0	11.7	2.374	4.022	0.733	−2.011	−3.864	−1.130	3.982
20.0	15.6	4.016	−0.801	1.387	2.304	−5.291	−0.906	3.408
20.0	19.5	3.952	2.023	−0.417	−0.443	−3.895	−1.077	2.997

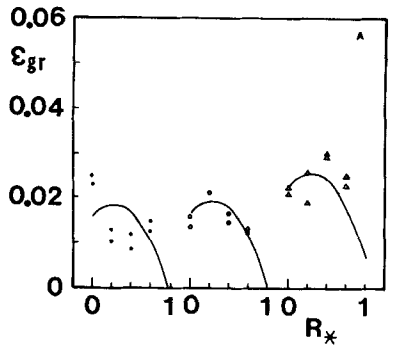

Figure 10a.

V_G = 12.8 mm/s; V_L = 3.9 mm/s
At Z = 0.075 m:
r/R = 0; ϵ_{gr} = 0.0752, 0.0820
r/R = 0.25; ϵ_{gr} = 0.0006, 0.0004
r/R = 0.5; ϵ_{gr} = 0.0017, 0.0026
r/R = 0.75; ϵ_{gr} = 0.0002, 0.0006

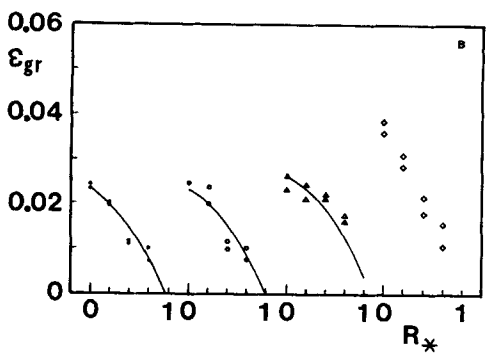

Figure 10b.

V_G = 12.8 mm/s; V_L = 7.9 mm/s
◊ in freeboard
At Z = 0.075 m:
r/R = 0; ϵ_{gr} = 0.0643, 0.0593
r/R = 0.25; ϵ_{gr} = 0.0133, 0.0169
r/R = 0.5; ϵ_{gr} = 0.0035, 0.0076
r/R = 0.75; ϵ_{gr} = 0.0008, 0.0023

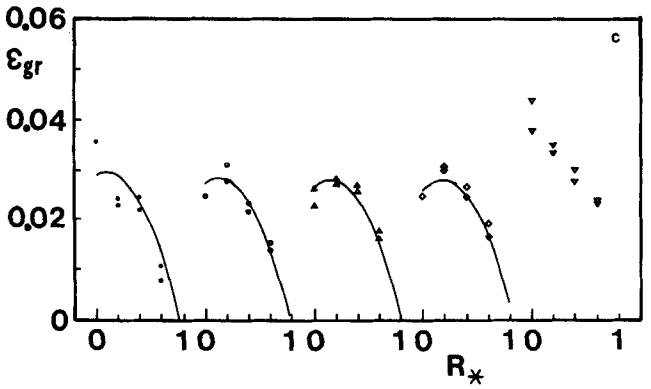

Figure 10c.

V_G = 12.8 mm/s; V_L = 11.7 mm/s
(▽) in freeboard
at Z = 0.075
r/R = 0; ϵ_{gr} = 0.0934, 0.0767
r/R = 0.25; ϵ_{gr} = 0.0078, 0.0103
r/R = 0.5; ϵ_{gr} = 0.0145, 0.0162
r/R = 0.75; ϵ_{gr} = 0.0029, 0.0042

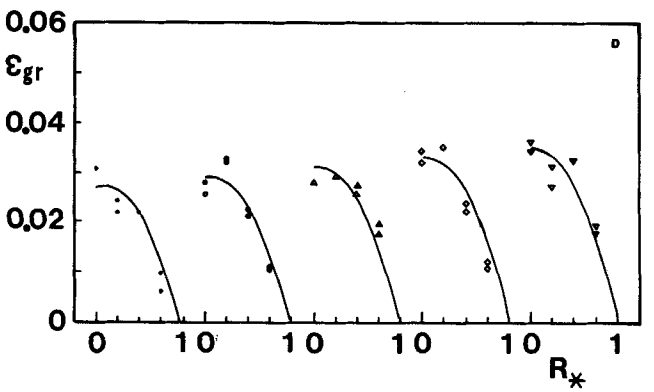

Figure 10d.

V_G = 12.8 mm/s; V_L = 15.6 mm/s
at Z = 0.075 m
r/R = 0; ϵ_{gr} = 0.0920, 0.0750
r/R = 0.25; ϵ_{gr} = 0.0078, 0.0133
r/R = 0.5; ϵ_{gr} = 0.0162, 0.0179
r/R = 0.75; ϵ_{gr} = 0.0028, 0.0044

Figure 10. Radial gas holdup profiles.

—Eq. 13 △ Z = 0.525 m
● Z = 0.225 m ◊ Z = 0.675 m
○ Z = 0.375 m ▽ Z = 0.825 m

results in an increasing tendency to bubble breakage. Consequently, smaller bubbles with lower rising velocities can be expected. Therefore, the gas holdup should increase, as was observed in the top section of the fluidized bed.

Some experiments were also performed in the freeboard region to demonstrate the effect of viscosity on bubble flow. Gas holdups in the freeboard are expected to be higher than those in the fluidized bed, as a result of lower viscosity in the two-phase region. It can be seen in Figure 10b that there is a noticeable increase of gas holdup in the freeboard even though the axial position is only about 1 cm above the fluidized bed. Such an increase is more noticeable for the case shown in Figure 10c, where the axial position of two-phase flow measurement is about 4 cm above the bed.

With the cross-sectional average gas holdup, the local pressure profile, and the relationship of continuity, the three-phase holdups in three-phase fluidized beds were studied at various operating conditions; the results are shown in Figure 11. The dashed lines in the figure represent the pseudobed height obtained from the conventional method of analysis using Eqs. 2, 3, and 4. It was observed that the solid and the liquid holdups remained quite constant in the lower part (approximately two-thirds) of the fluidized bed. In the upper part of the bed, the solid holdup decreased rapidly, while the liquid holdup increased correspondingly as the top of the bed was approached. The finding of an axial profile of solid holdup confirms the previous discussion about the axial distribution of gas holdup in the fluidized bed. In terms of gas holdup, there is an increasing tendency in the axial direction. However, the magnitude of change is much smaller than those of the solid and the liquid holdups. At the lowest axial position, Z = 0.075 m, the gas holdup is obviously lower than those at higher positions when low liquid

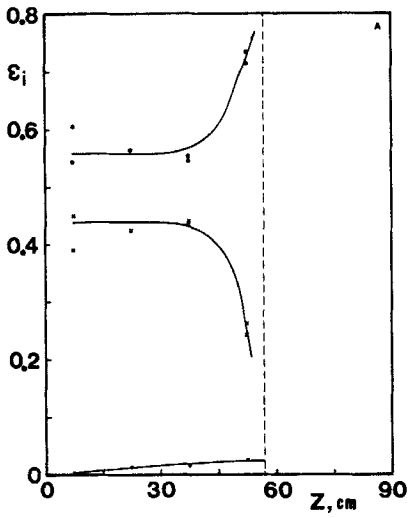

Figure 11a.

V_G = 12.8 mm/s; V_L = 3.9 mm/s

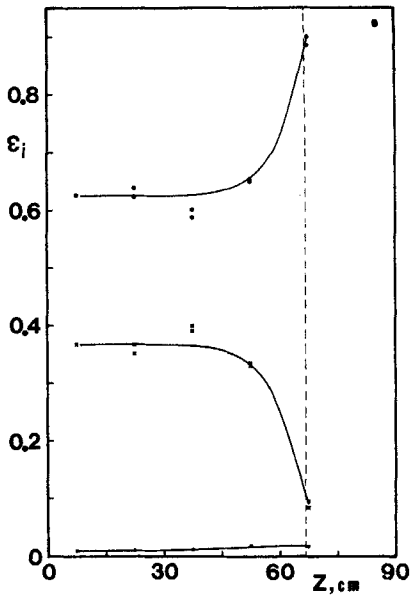

Figure 11b.

V_G = 12.8 mm/s; V_L = 7.9 mm/s

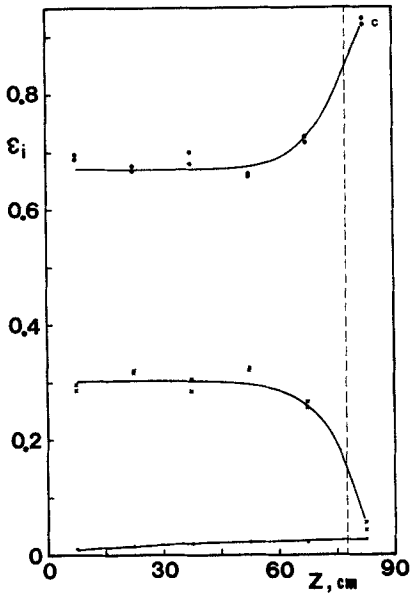

Figure 11c.

V_G = 12.8 mm/s; V_L = 11.7 mm/s

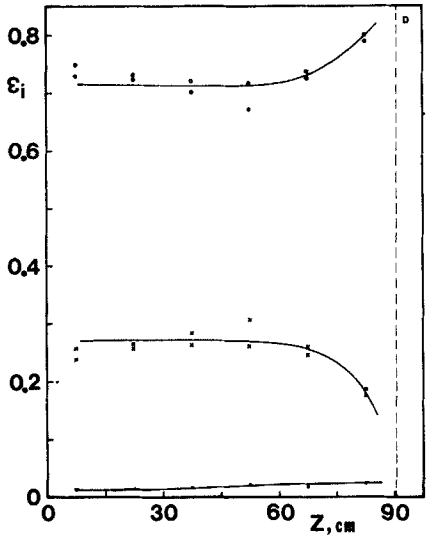

Figure 11d.

V_G = 12.8 mm/s; V_L = 15.6 mm/s

Figure 11.

Axial phase hold-up profiles

(●) gas phase (○) liquid phase (×) solid phase (---) pseudo bed heights

velocity is used. This phenomenon becomes less noticeable at higher liquid velocities.

In comparison with the conventional phase holdup analysis, the results obtained from the alternative method reveal, in general, similar observations. However, there are deviations between the results obtained from the two analyses. For example, the gas holdup computed by the conventional method is higher than that calculated by the other method. The discrepancy may be explained by the nature of the former method. After rearrangement of Eqs. 2, 3, and 4, it can be seen that a higher solid holdup results in a higher gas holdup if the same pressure profile is used. The assumption of lumping all the solid particles in a pseudobed is very likely to introduce error in the calculation of phase holdups. Since the particles used in this study are relatively small, it is inevitable that some particles are entrained and suspended in the freeboard. This could cause an overestimation of solid holdup and, consequently, of gas holdup. Certainly there is also some experimental error involved in the direct measurement of gas holdup. However, a mass balance of gas shown later in this paper indicates that the direct gas holdup measurement is fairly reliable.

The ability to measure gas holdup directly provides a way of

Table 3. Phase Holdups in the Freeboard

Run No.	Gas Veloc. mm/s	Liquid Veloc. mm/s	Three-phase Freeboard Gas Holdup	Three-phase Freeboard Liquid Holdup	Three-phase Freeboard Solid Holdup	Two-phase Freeboard Assumption Gas Holdup	Two-phase Freeboard Assumption Liquid Holdup
1	12.8	7.9	0.0171	0.982	0.001	0.0156	0.984
2	12.8	11.7	0.0263	0.965	0.009	0.0131	0.987
2	12.8	11.7	0.0263	0.968	0.005	0.0156	0.984
4	20.0	7.9	0.0356	0.961	0.004	0.0300	0.970
5	20.0	7.9	0.0356	0.962	0.002	0.0320	0.968

studying the entrainment of solid particles in the freeboard region. The technique described above for obtaining local phase holdups in the dense phase can also be applied to get the three holdups in the so-called two-phase region. In order to demonstrate the method, a few experiments in the freeboard immediately above the fluidized bed were performed. The gas holdup was measured by optical probes and an average solid holdup in the freeboard was calculated. Consequently, the liquid holdup in the freeboard was obtained. The results, listed in Table 3, indicate trends of particle entrainment. It can be seen in Table 3 that the solid holdup in the freeboard increases as either the gas or the liquid velocity is increased. Such a tendency can be expected and is understandable. In any case, it shows that the optical probe is a tool of very good potential in the study of particle entrainment in a three-phase fluidized bed.

The results of direct probe measurements showed that the gas holdup in the freeboard increased with increasing gas or liquid velocity. The effect of liquid velocity on gas holdup in the freeboard was consistent with the observations in a bubble column by Kim et al. (1972). If the assumptions of a two-phase (solid-free) freeboard is used, the gas and the liquid holdups can be obtained from the pressure profile in the freeboard. However, the results obtained are misleading, as shown in Table 3. Instead of increasing, the gas holdup appears to decrease with or to be independent of the liquid velocity. This is certainly a result of the two-phase freeboard assumption and such a simplification should not be made even though the amount of entrained particles is very small. Note that the fluidization velocities of the examples shown here are relatively low, V_G = 12.8 mm/s, V_L = 7.9 mm/s, and V_L = 11.7 mm/s. The error caused by the assumption of a solid-free freeboard will be even more pro-

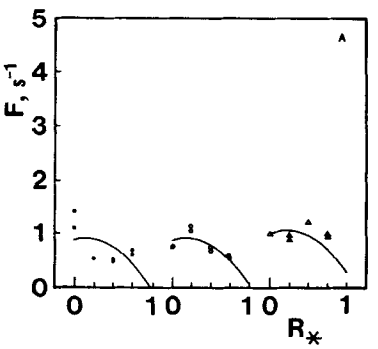

Figure 12a.

V_G = 12.8 mm/s; V_L = 3.9 mm/s
at Z = 0.075 m
r/R = 0; F = 4.63, 3.91; r/R = 0.25; F = 0.02, 0.02
r/R = 0.5; F = 0.12, 0.15; r/R = 0.75; F = 0.05, 0.01

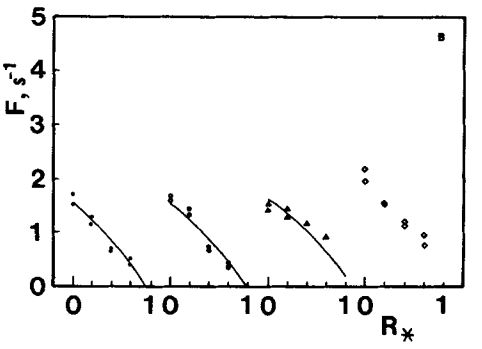

Figure 12b.

V_G = 12.8 mm/s; V_L = 7.9 mm/s
At Z = 0.075 m:
r/R = 0; F = 4.04, 3.38; r/R = 0.25; F = 0.75, 1.01
r/R = 0.5; F = 0.23, 0.43; r/R = 0.75; F = 0.05, 0.13
◇ in freeboard

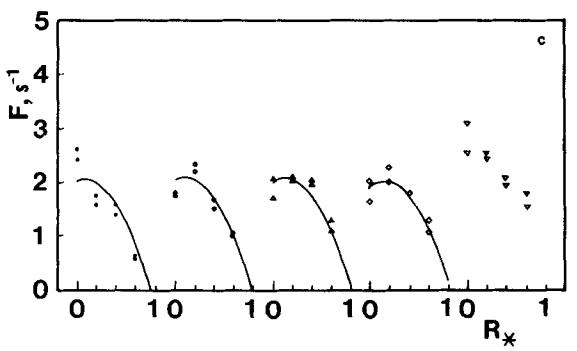

Figure 12c.

V_G = 12.8 mm/s; V_L = 11.7 mm/s
At Z = 0.075 m:
r/R = 0; F = 6.06, 4.77; r/R = 0.25; F = 0.49, 0.64
r/R = 0.5; F = 0.94, 0.99; r/R = 0.75; F = 0.20, 0.28
△ in freeboard

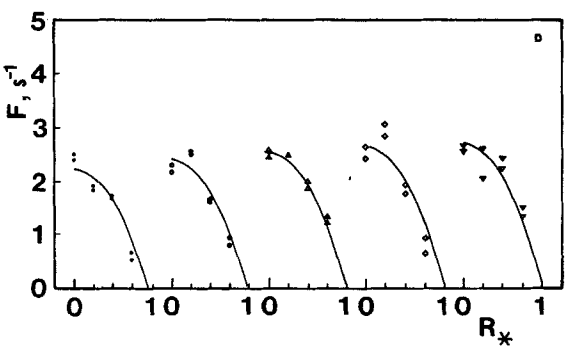

Figure 12d.

V_G = 12.8 mm/s; V_L = 15.6 mm/s
At Z = 0.075 m:
r/R = 0; F = 6.10, 4.78; r/R = 0.25; F = 0.55, 0.92
r/R = 0.5; F = 1.02, 1.05; r/R = 0.75; F = 0.23, 0.28

Figure 12. Radial bubble frequency profiles
(—) eq. 14
(●) Z = 0.225 m (○) Z = 0.375 m (△) Z = 0.525 m (◇) Z = 0.675 m (▽) Z = 0.825 m

Table 4. Response Surface Analysis of Bubble Frequency Profiles

$$F = b_1 + b_2 Z_* + b_3 R_* + b_4 Z_*^2 + b_5 R_*^2 + b_6 Z_* R_*$$

Gas Veloc. mm/s	Liquid Veloc. mm/s	b_1	b_2	b_3	b_4	b_5	b_6	Std. Dev. 1/s
12.8	3.9	1.168	−1.125	0.300	1.009	−1.390	0.382	0.213
12.8	7.9	1.845	−1.255	−1.370	1.216	−0.503	0.571	0.150
12.8	11.7	1.928	0.514	0.249	−0.657	−2.799	0.952	0.214
12.8	15.6	1.900	1.463	0.175	−0.636	−2.582	−0.232	0.220
20.0	3.9	2.189	−3.069	0.219	2.570	−1.733	0.342	0.269
20.0	7.9	0.670	5.172	−0.259	−4.040	−1.670	−0.325	0.152
20.0	11.7	1.612	3.436	−0.056	−2.285	−2.461	−0.251	0.255
20.0	15.6	2.610	1.717	0.581	−0.265	−3.650	−0.731	0.228
20.0	19.5	2.553	4.858	−0.332	−2.510	−2.937	−2.052	0.252

nounced at higher fluidization velocities due to higher solid entrainments.

An example of the bubble frequency profiles in the fluidized bed is shown in Figure 12. Similar results were also obtained for other operating conditions (Lee, 1986). The response surface method was also applied to study the bubble frequency profiles both axially and radially in the fluidized beds. The dimensionless axial and radial positions were considered to be the two independent variables in the model. The format of the model used is shown in the following equation:

$$F = b_1 + b_2 Z_* + b_3 R_* + b_4 Z_*^2 + b_5 R_*^2 + b_6 Z_* R_* \quad (14)$$

The experimental data obtained under different operation conditions were analyzed separately. The results of the analyses are listed in Table 4, which includes the various coefficients and the standard deviations.

It was found that the gas holdup was very closely related to the bubble frequency. As a matter of fact, the trends observed in the study of bubble frequency were also found in the investigation of gas holdup. Such a finding may be explained considering the observation of bubble velocity and bubble length distribution. It can certainly be understood that the gas holdup is influenced by the bubble frequency and the durations of detected bubbles. The duration of a particular bubble can be represented by the ratio of its axial length and its rising velocity. Since there is a certain relationship between the bubble velocity and the bubble length, the duration of a certain bubble length can be obtained. In addition, a unique bubble length distribution exists under a certain operating condition. With these factors in mind, a duration distribution can be established for a particular operating condition. Therefore, it can be expected that the gas holdup is directly proportional to the bubble frequency, with the average bubble duration as the proportionality factor. This factor may be slightly different for various conditions due to the change in bubble length distribution and consequently the average bubble duration. These speculations may offer an explanation for the similarities observed.

In any case, the gas holdup and the bubble frequency provide identical information, however in different forms. The preference for one form over the other depends on the convenience of use. For some particular phenomena the gas holdup provides a clear picture for observation. This is due to the amplification effect of translating the bubble frequency into the gas holdup. For example, the sudden increase of gas holdup near the top of the bed is more pronounced than the observation of bubble frequency under the same conditions.

The average bubble velocity was assessed by using a cross-correlation technique. Measurements were performed at various locations in the three-phase fluidized beds. An example of the results is listed in Table 5. Results for other operating conditions can be seen in Lee (1986).

The ability to measure local average bubble velocity provides the possibility of performing a gas mass balance that can be used to check the accuracy of the measuring technique. This also requires the information of local gas holdups. The balance is based on the assumption of symmetrical gas flow in the angular direction. At a fixed axial position, a cross-sectional average superficial gas velocity can be calculated by the following equation:

$$V_{gc} = \frac{1}{\pi R^2} \int_0^R V_r \epsilon_{gr} 2\pi r \, dr \quad (15)$$

where V_{gc} is the cross-sectional average superficial gas velocity, V_r is the local average bubble velocity, ϵ_{gr} is the local gas holdup, r is the radial position, and R is the radius of the column. The superficial gas velocity calculated by Eq. 15 can be compared to the actual superficial gas velocity, which is set by the operating

Table 5. Average Bubble Velocities in Three-Phase Fluidized Bed, cm/s

Axial Position m	Radial Position, R_* 0	0.25	0.50	0.75
0.825	78.3	78.3	67.1	47.0
	(76.5)	(76.4)	(67.2)	(44.5)
0.675	78.3	67.1	58.8	58.8
	(75.1)	(64.5)	(58.6)	(53.8)
0.525	78.3	67.1	67.1	58.8
	(75.4)	(67.9)	(64.9)	(59.9)
0.375	78.3	67.1	67.1	47.0
	(76.2)	(65.8)	(64.5)	(48.8)
0.225	67.1	67.1	58.8	58.8
	(65.2)	(63.9)	(62.1)	(53.2)
0.075	67.1	58.8	58.8	67.1
	(67.7)	(58.6)	(61.8)	(64.0)

Gas velocity = 20.0 mm/s
Liquid velocity = 19.5 mm/s.
*Bubble velocities are obtained through either cross correlation or phase angle and the results of the latter method are shown within parentheses.

Table 6. Mass balance of gas phase; % Error of Calculated Gas Velocity with Respect to Actual Superficial Gas Velocity

Gas Veloc. mm/s	Liquid Veloc. mm/s	Axial Position, m					
		0.075	0.225	0.375	0.525	0.675	0.825
12.8	3.9	−70.65	−36.59	−19.92	11.77	—	—
12.8	7.9	−48.78	−33.23	−44.26	−12.65	—	—
12.8	11.7	−23.26	−16.00	−7.20	7.37	−10.17	(1.42)
12.8	15.6	−18.01	−12.81	−9.69	23.55	11.26	16.73
20.0	3.9	−64.18	−25.51	−22.59	1.77	—	—
20.0	7.9	−57.04	−36.16	−20.80	−26.03	(2.64)	—
20.0	11.7	−17.61	−8.31	−10.29	1.61	−10.14	—
20.0	15.6	4.88	−12.62	−5.74	0.65	−2.20	17.05
20.0	19.5	10.10	−14.69	−1.70	5.79	−0.23	5.12

Results in parentheses are from freeboard region.

condition. Note that the actual gas velocity has to be corrected according to the static pressure at the axial position of interest. The comparison between the calculated and the actual gas velocities at various conditions is shown in Table 6. The results of two experiments in the freeboard region are also reported within parentheses in Table 6.

The results show that better agreement between the calculated and the actual velocities exists when a higher liquid-gas velocity ratio is used. This observation can be explained by the hydrodynamic flow patterns in fluidized beds. A high liquid velocity results in small gas bubbles and high bubble frequency. Under this condition, the signals detected by the probes exhibit more characteristics of random data and are closer to the hypothesis of stationarity. Therefore, the signals obtained are more suitable for statistical analysis. On the other hand, there is more deviation from the stationary random data assumption in signals obtained under a low liquid-gas velocity ratio. Hence, better results can be observed at conditions with a higher liquid-gas ratio. In summary, the agreement between the calculated and the actual velocities is quite reasonable. This is particularly true for most of the experiments performed at axial levels of 0.225 m and higher where the assumption of flow symmetry applies.

Acknowledgment

Support from the Natural Sciences and Engineering Research Council of Canada (NSERC) is gratefully acknowledged.

Notation

a_1–a_6 = coefficients, Eq. 13
A = cross-sectional area of fluidized bed, cm^2
b_1–b_6 = coefficients, Eq. 14
F = bubble frequency, Eq. 14, 1/s
g = gravitional acceleration, m/s^2
H_b = fluidized bed height, m
M_s = total weight of solid particles, kg
P = static pressure at height, Z, kPa
r = radius, m
R = radius of fluidized bed, m
R_* = radius, r/R
T = sampling time, s
V_G = superficial gas velocity, cm/s
V_{gc} = superficial gas velocity, Eq. 15, cm/s
V_L = superficial liquid velocity, cm/s
V_r = average bubble velocity at radius r, cm/s
Z = height, m
Z_* = height, Z/H_b

Greek letters

ϵ = bed porosity, $\epsilon_l + \epsilon_g$
ϵ_{gr} = local gas holdup at r and Z
ϵ_l, ϵ_g, ϵ_s = local liquid, gas, and solid holdups at Z
ϵ_L, ϵ_G, ϵ_S = global liquid, gas, and solid holdups
ρ_L, ρ_G, ρ_S = density of liquid, gas, and solid phases, kg/m^3
$\triangle P$ = pressure drop across fluidized bed, kPa
$\triangle t_i$ = time corresponds to the period a bubble contacts the probe(s)

Literature Cited

Armstrong, E. R., C. G. J. Baker, and M. A. Bergougnou, "The Effects of Solids Wettability on the Characteristics of Three-Phase Fluidization," *Fluidization Technology*, D. L. Keairns, ed., Hemisphere, Washington, DC, 453. (1976).

Baker, C. G. J., "Three-Phase Fluidization," *Multiphase Chemical Reactors*, S. A. Rodrigues, J. Calo, and N. Sween, eds., Stihoff and Noordhoff, The Netherlands, 343 (1981).

Baker, C. G. J., S. D. Kim, and M. A. Bergougnou, "Wake Characteristics of Three-Phase Fluidized Beds," *Powder Technol.*, **18**, 201 (1977).

Begovich, J. M., "Hydrodynamics of Three-Phase Fluidized Beds," Oak Ridge Nat. Lab. Rept. No. ORNL/TM-6448 (1978).

Begovich, J. M., and J. S. Watson, "An Electroconductivity Technique for the Measurement of Axial Variation of Holdups in Three-Phase Fluidized Beds," *AIChE J.*, **24**, 351 (1978a).

———, "Hydrodynamic Characteristics of Three-Phase Fluidized Beds," *Fluidization, Proc. 2nd Eng. Found. Conf.*, Cambridge, 190 (1978b).

Bendat, J. S., and A. G. Piersol, *Measurement and Analysis of Random Data*, Wiley, New York (1966).

———, *Engineering Applications of Correlation and Spectral Analysis*, Wiley, New York (1980).

Bhatia, V. K., and N. Epstein, "Three-Phase Fluidization: A Generalized Wake Model," *Fluidization and its Application*, Toulouse, France, 380 (1974).

Bhatia, V. K., K. A. Evans, and N. Epstein, "Effect of Solids Wettability on Expansion of Gas-Liquid Fluidized Beds," *Ind. Eng. Chem. Process Des. Dev.*, **11**(1), 151 (1972).

Bickel, T. C., and M. G. Thomas, "Catalyst Deactivation in the H-Coal Coal Liquefaction Process. 1: Catalyst Residence Time Distribution," *Ind. Eng. Chem. Process Des. Dev.*, **21**, 377 (1982).

Blum, D. B., and J. J. Toman, "Three-Phase Fluidization in a Liquid Phase Methanator," *AIChE Symp. Ser.*, **161**(73), 115 (1977).

Dakshinamurty, P., V. Subrahmanyam, and J. N. Rao, "Bed Porosities in Gas-Liquid Fluidization," *Ind. Exp. Chem. Process Des. Dev.*, **10**, 322 (1971).

Dakshinamurty, P., D. V. Rao, R. V. Subbaraju, and V. Subrahmanyam, "Bed Porosities in Gas-Liquid Fluidization," *Ind. Eng. Chem. Process Des. Dev.*, **11**, 318 (1972).

Darton, D. C., and D. Harrison, "Bubble Wake Structure in Three-Phase Fluidization," *Fluidization Technology*, Hemisphere, Washington, DC, 399 (1976).

Deckwer, W. D., "FT Process Alternatives Hold Promise," *Oil & Gas J.*, 198 (Nov. 10, 1980).

de Lasa, H., S. L. P. Lee, and M. A. Bergougnou, "Bubble Measurement in Three-Phase Fluidized Beds Using a U-shaped Optical Fiber," *Can. J. Chem. Eng.*, **62**(2), 165 (1984).

de Lasa, H. I., and S. L. P. Lee, *Three-Phase Fluidized-Bed Reactors*, H. I. de Lasa, ed., Martinus-Nijhoff, The Netherlands, 349 (1986).

Dhanuka, V. R., and J. B. Stepanek, "Gas and Liquid Holdup and Pressure Drop Measurements in a Three-Phase Fluidized Bed," *Fluidization*, Cambridge, 179 (1978).

Efremov, G. I., and I. A. Vakhrushev, "A Study of the Hydrodynamics of Three-Phase Fluidized Beds," *Int. Chem. Eng.*, **10**(1), 37 (1970).

El-Temtamy, S. A., and N. Epstein, "Bubble Wake Solids Content in Three-Phase Fluidized Beds," *Int. J. Multiph. Flow*, **4**, 19 (1978).

Epstein, N., "Three-Phase Fluidization: Some Knowledge Gaps," *Can. J. Chem. Eng.*, **59**, 649 (1981).

Hellwig, K. C., et al., "Make Liquid Fuels from Coal," *Hydrocarb. Process.*, 165 (May, 1966).

Hu, T. T., B. T. Yu and Y. P. Wang, "Holdups and Models of Three Phase Fluidized Beds," Fluidization V., Eds. K. Ostergaard and A. Sorensen, Engr. Found., New York, 353 (1986).

Kim, S. D., C. G. J. Baker, and M. A. Bergougnou, "Holdup and Axial Mixing Characteristics of Two- and Three-Phase Fluidized Beds," *Can. J. Chem. Eng.*, **50**, 695 (1972).

———, "Phase Holdup Characteristics of Three-Phase Fluidized Beds," *Can. J. Chem. Eng.*, **53**, 134 (1975).

Lee, S. L. P., "Bubble Dynamics in Three-Phase Fluidized Beds," Ph.D. Diss. Univ. Western Ontario, London, Canada (1986).

Lee, S. L. P., H. I. de Lasa, and M. A. Bergougnou, "Bubble Phenomena in Three-Phase Fluidized Beds as Viewed by a U-shaped Fiber Optic Probe," *AIChE Symp. Ser.*, **80**(241), 110 (1984).

———, "A U-shaped Fiber Optic Probe to Study Three-Phase Fluidized Beds," *Particle Sci. Technol.*, **4**, 61, 1986.

Linneweber, K. W., and E. Blass, "Measurement of Local Gas and Solids Holdups in Three-Phase Bubble Columns," *Ger. Chem. Eng.*, **6**, 28 (1983).

Morooka, S., K. Uchida, and Y. Kato, "Recirculating Turbulent Flow of Liquid in Gas-Liquid-Solid Fluidized Bed," *J. Chem. Eng. Japan*, **15**(1), 29 (1982).

Mounce, W., and R. S. Rubin, "The H-Oil Route for Hydroprocessing," *Chem. Eng. Prog.*, 81 (Aug., 1971).

Muroyama, K., and L. S. Fan, "Fundamentals of Gas-Liquid-Solid Fluidization," *AIChE J.*, **31**, 1 (1985).

Ostergaard, K., "On Bed Porosity in Gas-Liquid Fluidization," *Chem. Eng. Sci.*, **20**, 165 (1965).

———, "Three-Phase Fluidization," *Fluidization*, J. F. Davidson and D. Harrison, eds., Academic Press, New York, 751 (1971).

Rapp, L. M., and R. P. van Driesen, "H-Oil Process Gives Product Flexibility," *Hydrocarb. Process.*, 103, (Dec., 1965).

Razumov, I. M., V. V. Manshilin, and L. L. Nemets, "The Structure of Three-Phase Fluidized Bed," *Int. Chem. Eng.*, **13**(1), 57 (1973).

Razumov, I. M., V. V. Manshilin, L. L. Nemets, L. M. Zin'kov, and N. I. Terekhov, "Calculation of Expansion of Three-Phase Fluidized Bed," *Chem. Tech. Fuels Oils* (USSR), **13**(7/8) 506 (1977).

Rigby, G. R. and C. E. Capes, "Bed Expansion and Bubble Wakes in Three-Phase Fluidization," *Can. J. Chem. Eng.*, **48**, 343 (1970).

Smith, E. L., A. James, and M. Fidgett, "Fluidization of Microbial Aggregates in Tower Fermenters," *Fluidization*, 196 (1978).

Soung, W. Y., "Bed Expansion in Three-Phase Fluidization," *Ind. Eng. Chem. Process Des. Dev.*, **17**(1), 33 (1978).

Vail, Y. K., N. K. Manakov, and V. V. Manshilin, "The Gas Contents of Three-Phase Fluidized Beds," *Int. Chem. Eng.*, **10**(2), 244 (1970).

Wild, G., "Les Reacteurs a lits fluidise gas-liquide-solide. Etat de l'art et perspectives industrielles," *Entropie*, **3**, 1983.

Manuscript received Aug. 11, 1986, and revision received Feb. 2, 1987.